P8.14 CLASSIC AND HP MINI-SUPERCELLS IN SOUTHEAST OREGON AND SOUTHWEST IDAHO ON 3 MAY 2009

Stephen S. Parker*
National Weather Service, Boise, ID

1. INTRODUCTION

During the early afternoon hours of 3 May 2009, severe thunderstorms formed in southeast Oregon and southwest Idaho in advance of a strong short-wave trough. Two of these storms displayed characteristics of mini-supercells (Burgess, et al. 1995) - one classic in structure and one High Precipitation (HP). The classic mini-supercell displayed an unusual mesocyclone occlusion, a large three-body scatter spike, and an obvious rear-flank downdraft (RFD). The HP mini-supercell displayed a pronounced kidney-bean shape, a moderate mid-level mesocyclone, large weak echo region (WER) and a sharp movement to the right of the mean wind. These storm structures are rare in this part of the country, owing largely to insufficient low-level moisture and high CCL (Hurlbut and Parker, 2006). This paper will seek to describe in detail both environmental pre-storm conditions and storm structure and evolution determined from radar. The goals are: to increase understanding of the atmospheric conditions conducive to these storm types in this climatic region; to increase local recognition of these storm structures by documenting local examples; and therefore to increase situational awareness of future similar events.

Corresponding Author: Stephen S. Parker
NOAA/NWS 3833 S. Development Ave., NIFC Bldg 3807
Boise, ID 83705-5354 (208) 334-9508
email: Stephen.Parker@noaa.gov

2. SYNOPTIC AND MESOSCALE OVERVIEW

A strong short-wave trough was moving east through the Pacific Northwest during the morning of 3 May 2009. This helped increase instability and aided in initiating thunderstorms in southeast Oregon and southwest Idaho in the late morning hours (around 1700 GMT, or 11 am MDT). The darkening across northern CA indicates the presence of a jet streak.

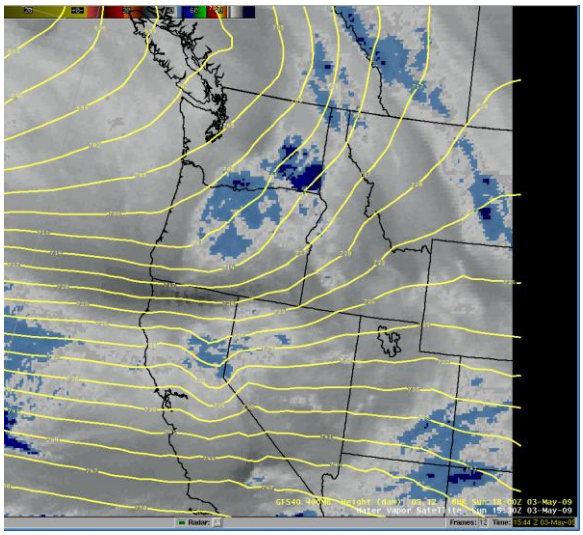

Figure 1. 15Z 3 May 2009 Water Vapor image showing a well-defined short-wave trough approaching southeast Oregon and southwest Idaho.

The 12Z sounding from Boise, ID (not shown) was ahead of the trough and was contaminated by light shower activity. The atmosphere ahead of the short-wave trough changed rapidly, and is best depicted by plan-view model data because the pre-selected BUFR sounding sites failed to capture the maxima in the important fields. The complex terrain in this area occasionally renders

the pre-selected BUFR points minimally useful. In this case, the BUFR points simply missed the maximum values because they were small-scale features. The terrain is shown in Figure 2. This will help orient the reader for the subsequent plan-view images.

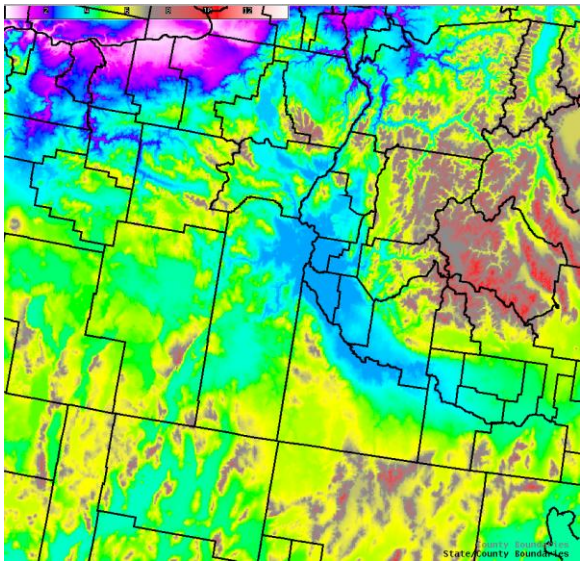

Figure 2. Topographic image of eastern Oregon, southwest Idaho, and northern Nevada. Values are in thousands of feet.

Positive Buoyant Energy (Jkg^{-1}) from the 12Z NAM valid at 18Z (Fig. 3) shows an enhanced ribbon of instability (the darker blue area in Fig 3) extending along the southern end of the Treasure Valley (the medium blue area near the center of Fig.2). Both storms that we will discuss initiated in the western end of this maximum. The maximum drifted northeast by 21Z (Fig 4).

Although these values may seem small compared with typical supercell environments east of the Rockies, the majority of the severe weather in southeast Oregon and southwest Idaho seems to occur with less than 1000 Jkg^{-1} of positive buoyant energy. With the short-wave trough moving in, shear increased and was more than adequate to support highly organized convection.

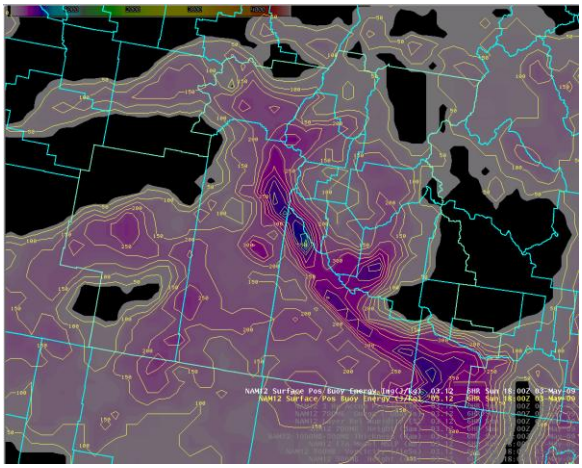

Figure 3. Positive Buoyant Energy from the 12Z run of the NAM valid at 18Z. Darker blue values indicate maxima. The classic mini-supercell initiated in the western portion of the maximum in the center of this image.

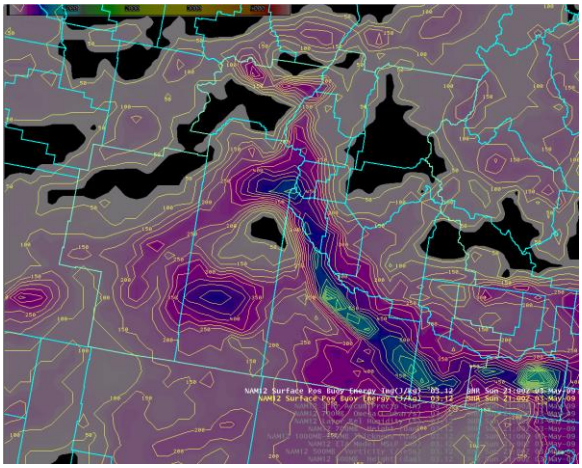

Figure 4. As in Figure 3, but for 21Z. The maximum in the center of the image has drifted northeast.

The Storm Relative Environmental Helicity (SREH) in the 0-3 km layer from the 12Z NAM valid at 18Z (Fig 5) showed a maximum just to the southwest of where the storms developed. By 21Z (Fig 6) this maximum had progressed northeast through the area where the storms attained their strongest signatures.

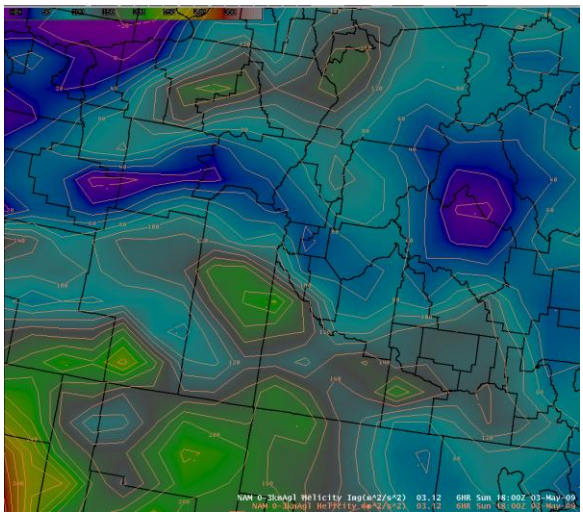

Figure 5. SREH in the 0-3 km layer from the 12Z NAM valid at 18Z. Note the maximum closest to the center of the image (green color with values over 200 m^2s^{-2}).

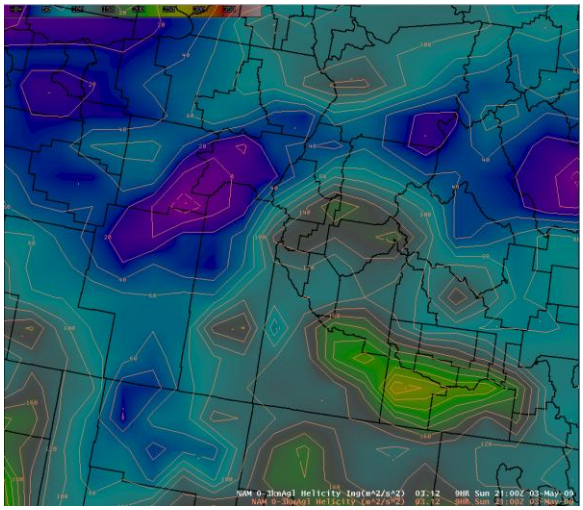

Figure 6. As in Figure 5, but valid at 21Z. Maximum near the center of the image is now around 170 m^2s^{-2}.

3. STORM STRUCTURE AND EVOLUTION

3a). Classic Mini-Supercell

Of the two storms, the storm that became a classic mini-supercell formed first. Initial detectable echo was at 1600Z, but it was small until 1733Z. The storm then developed rapidly, and by 1756Z it had a pronounced three-body scatter spike (TBSS) as shown in Fig 7a (4-panel of base reflectivity). The corresponding SRM 4-panel is shown in Fig 7b.

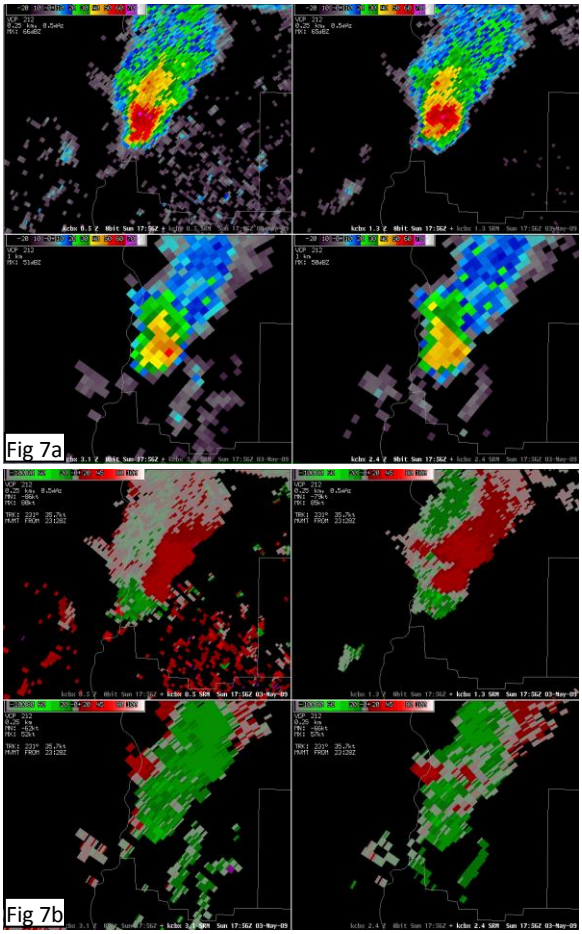

Figure 7. a). The top image is a 4-panel of base reflectivity from KCBX at 1756Z on 3 May 2009. The angles are 0.5, 1.3, 2.4, and 3.1 degrees, going clockwise from top-left to bottom- left. The radar is to the southeast and the TBSS is seen extending out of the northwest side of the echo at 0.5 and 1.3 degrees. b). Same as a) but for SRM.

The size of the cell is clearly "mini". In Fig.7a, top left hand panel, the red portion of the cell is approximately 8 km (4.5 nm) in the northeast - southwest direction, and about 6 km (3.2 nm) in the northwest - southeast direction. Cell top averaged around 9 km (29.5 kft).

On the next page, similar images from 1805Z, 1824Z, 1833Z, and 1838Z are displayed. These will be referred to as Figures 8 (a and b) through 11 (a and b).

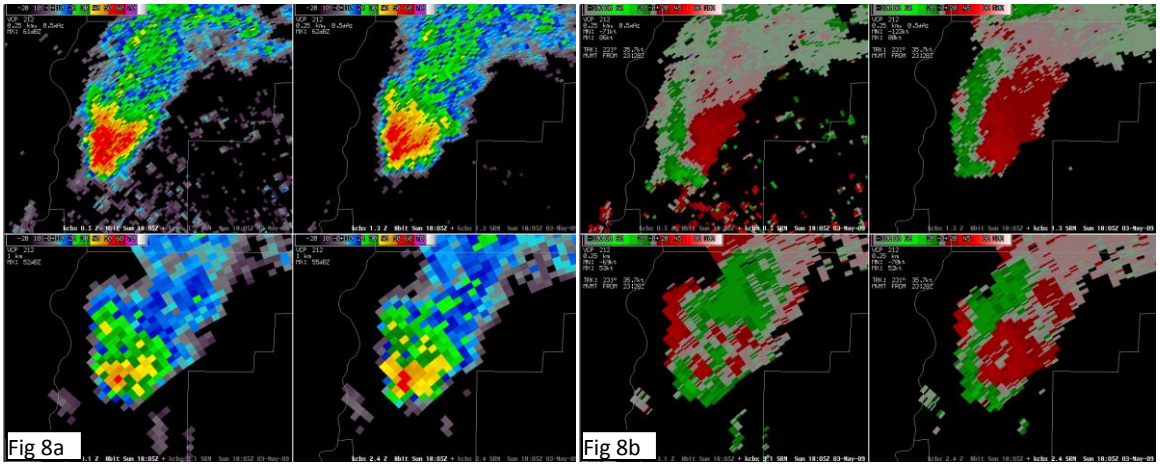

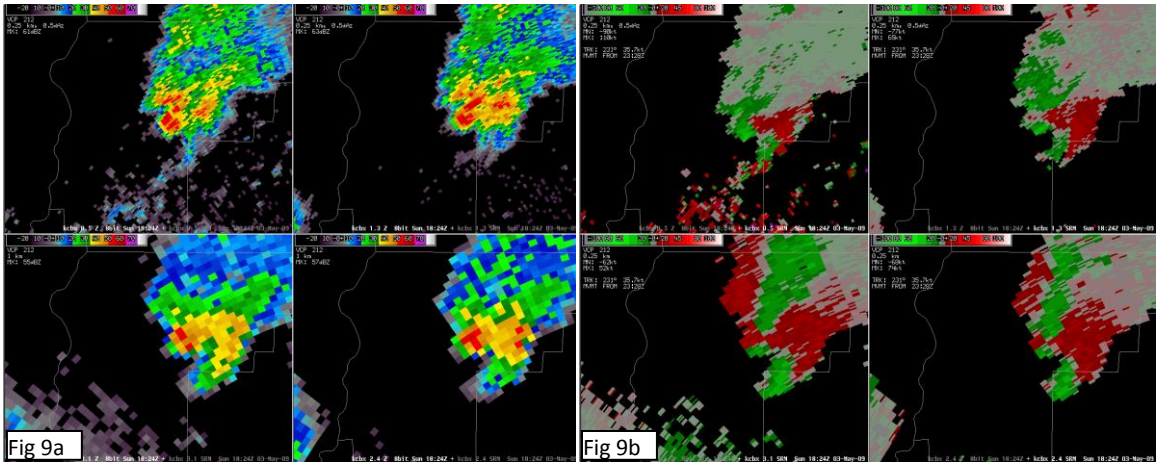

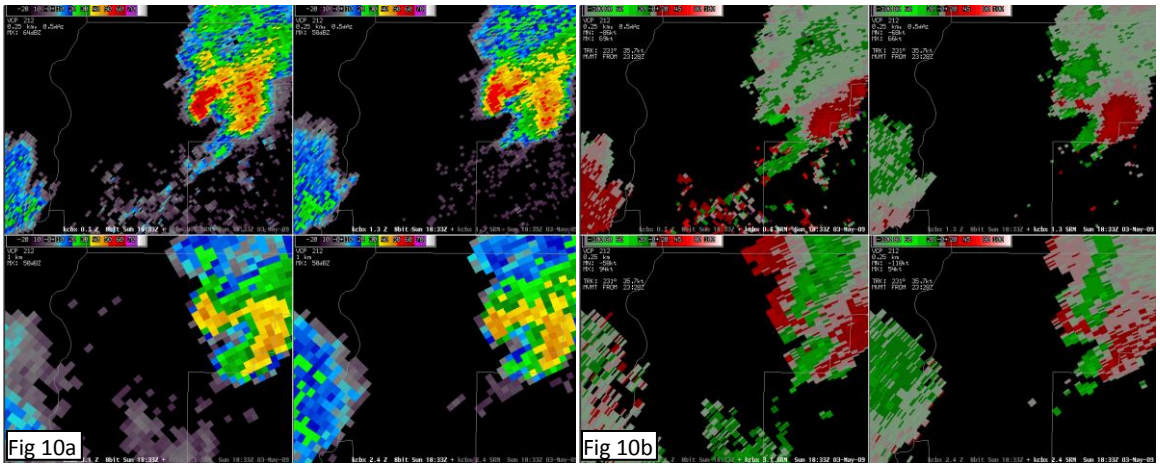

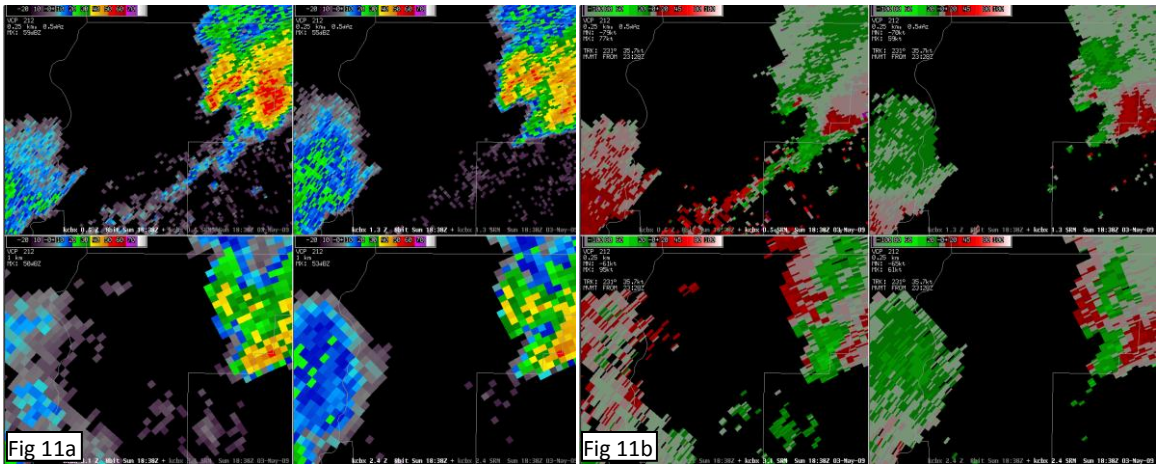

Figures 8 through 11 (a and b). As in Figure 7 but for 1805Z, 1824Z, 1833Z, and 1838Z.

This storm underwent an atypical evolution. It rapidly strengthened and became severe around 25 minutes after first echo. Then the storm began to shrink in size and develop a two-core structure aloft (Fig 9). At this time (1825Z) it also showed the beginnings of a rear-flank downdraft (RFD) boundary extending southwestward from the main core. There was significant rotation in the larger and "older" core on the west side of the storm, while the new core forming to the east displayed some shear as well. This marked the beginning of the mesocyclone occlusion process.

By 1833Z (Fig 10), the older core displayed an increase in reflectivity values and exhibited a tight small-scale rotation at the lowest level. The two cores were more clearly separated at this time. Only five minutes later (Fig 11), the older core had weakened significantly while the new core to the east underwent a corresponding amount of strengthening. The small-scale tight rotation in the older core remained at this time, but disappeared by the following volume scan. As the occlusion process neared an end, the RFD became associated with the newer core (the change is most obvious when comparing figures 9 and 11).

Throughout this portion of the evolution, the storm remained away from spotters. Therefore we have no official severe weather reports. However, by comparing the structure and reflectivity at this time with those associated with later reports from the storm, it appears likely that hail to around 1 inch in diameter was occurring during this time period. There was also a report of a funnel cloud at 1830Z from a spotter about 15 km (9 miles) southeast of the storm. This report, combined with the tight low-level velocity signature, prompted a tornado warning. After the storm, there was no evidence that a tornado touched down, but the population density of the area is low enough to leave doubt.

The new core went on to produce hail to one inch in diameter, and existed for several more hours. There were no additional mesocyclone occlusions with this cell.

3b). High Precipitation Mini-Supercell

The second storm formed in the same area as the first one, but about two hours later. It was approximately the same size. Figures 12 through 19 (a and b) show this storm at 1933Z, 1949Z, 1954Z, 2008Z, 2013Z, 2017Z, 2022Z, and 2026Z, respectively. First echo was at 1842Z. Rapid intensification began at 1924Z and occurred as it was merging with a small shower (not shown). By 1933Z (Fig 12 a and b), the storm had intensified and taken on a structure aligned along the low-level wind-shear vector, with a forward tilt with height. Moderate rotation developed by 1949Z (Fig 13 a and b). What had been a forward flank notch in the time between figures 12 and 13 became wrapped up into what can best be described as a letter "c" shape by 1954Z (Fig 14a, seen in the lowest two elevations angles). An interesting feature is seen at 1.3 degrees in Fig 14b - a band of outbound velocities that extends from just southeast of the mesocyclone to the south-southwest. This feature wraps directly into the mesocyclone, and represents air being lifted over the outflow from the flanking line to the south of the cell. This likely would have enhanced SREH and helped the storm maintain supercellular characteristics.

By 2008Z (Fig. 15 a and b), the "c" shape had diminished and the cell was reorganizing into a High Precipitation (HP) mini-supercell. From that time until the final image (Fig 19 a and b) at 2026Z, the storm moved due east and displayed a large forward flank notch with the strongest reflectivities immediately behind the notch (in a storm-motion-relative sense). The strongest reflectivities aloft were directly above the low-level notch – forming a large WER and clearly showing the position of the updraft. At 2026Z, the velocity images show a region of shear associated with the updraft, but no couplet such as that seen at 1949Z and 1954Z (Figs 13b and 14b).

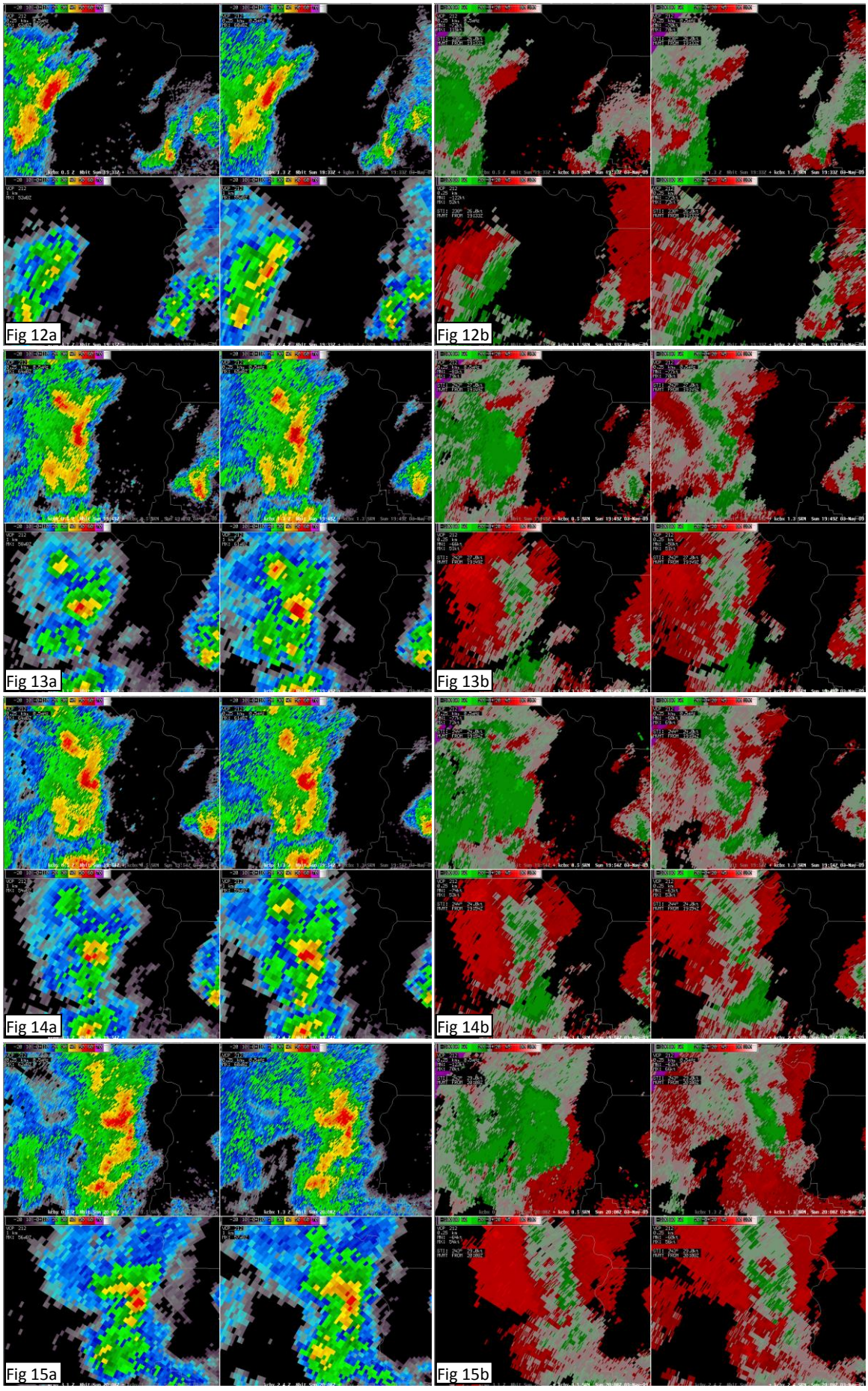

Figures 12 through 15 (a and b). As in Figure 7, but for 1933Z, 1949Z, 1954Z, and 2008Z.

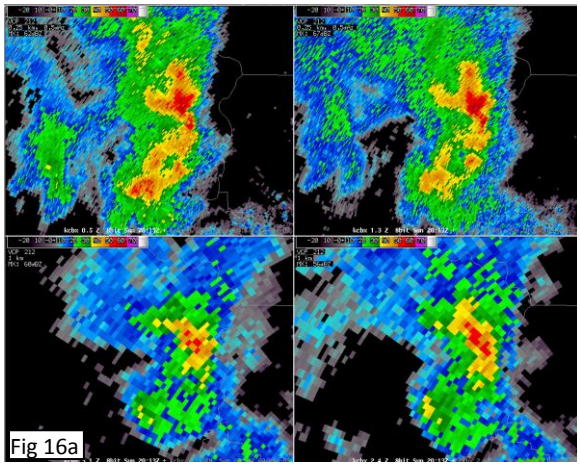

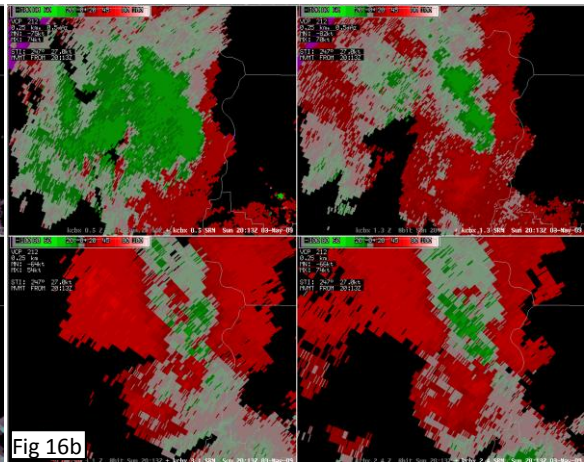

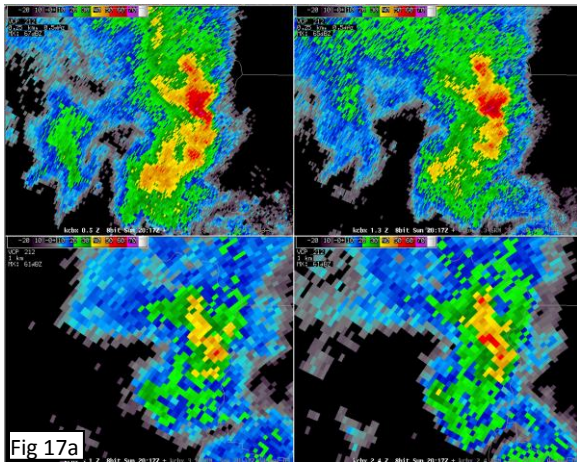

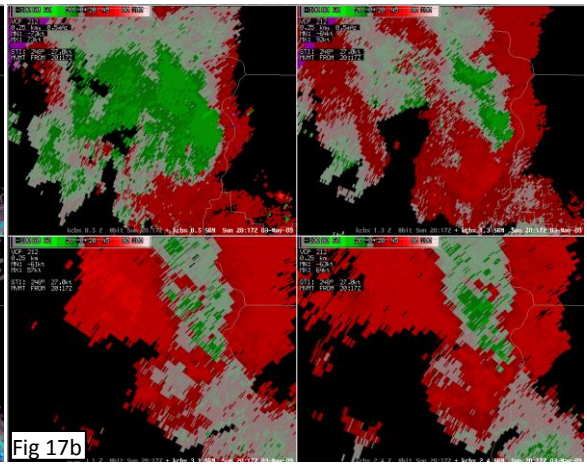

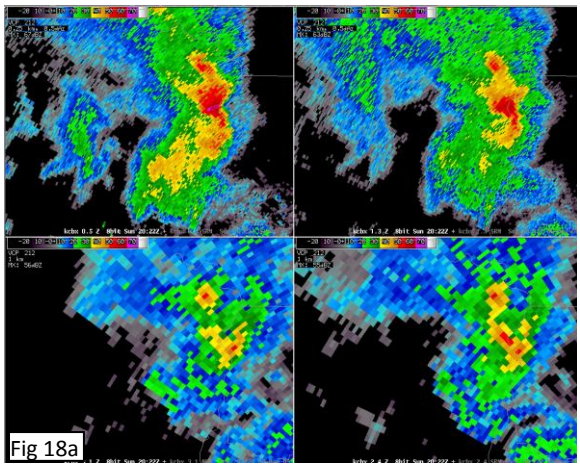

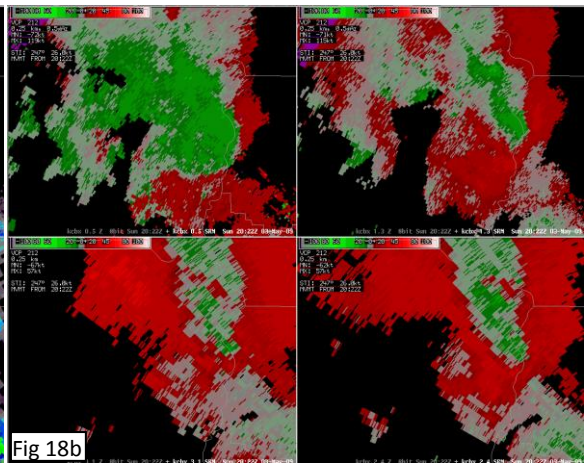

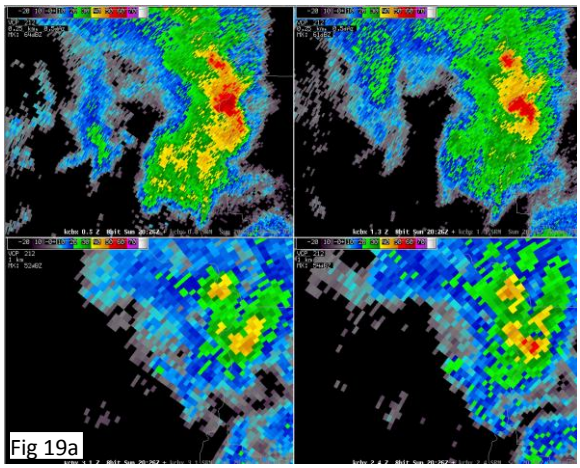

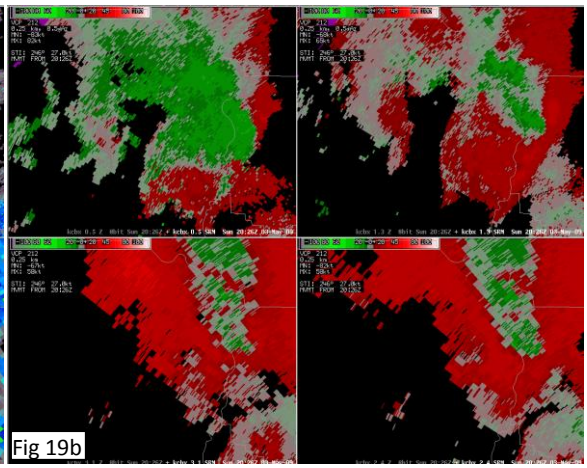

Figures 16 through 19 (a and b). As in Figure 7, but for 1933Z, 1949Z, 1954Z, and 2008Z.

4. DISCUSSION AND CONCLUSIONS

The occurrence of two mini-supercells in southeast Oregon and southwest Idaho is rare. Although there is often sufficient shear, there is seldom sufficient low-level moisture to support these structures. On 3 May 2009, we had both. The storm referred to as a classic mini-supercell displayed an unusual mesocyclone occlusion. The occluding rotation tightened rapidly as it experienced one last updraft pulse (as evidenced by the rapid increase and decrease in reflectivities from 1824Z to 1838Z, figures 9a through 11a). This occurred well behind the RFD, and the source for the updraft pulse is not known. It does not appear to be related to topography, as the storm was over relatively flat ground at the time. The author is interested in seeing other examples of similar evolutions. Please contact him if you know of any.

After the final image, this storm went on to produce one-inch diameter hail. It became nearly stationary as it encountered higher topography to the northeast. It continued to rotate weakly for about two more hours, but did not take on the classic mini-supercell characteristics that it had before.

The most organized storm of the day, the HP mini-supercell, was only able to sustain this structure for about 30 minutes. We suspect that this was aided by storm-relative inflow moving along the leading edge of the flanking line to the south and bringing high SREH air to the updraft. It may also have been aided by a boundary left by the previous storm. We have seen many instances of HP supercells forming along the outflow boundary of a previous storm, with the notch in the HP supercell co-located with the boundary. However, we lack the detailed observations necessary to determine if it occurred In this case.

At its strongest, the storm remained over open country, and no severe weather reports were received. Therefore we do not know if there was large hail or strong winds. However, with the limited information we did receive on this day, we believe it produced hail to around one inch in diameter.

We believe that the frequent reorganization seen in this storm (such as the transition from forward flank notch to "c" shape to HP mini-supercell) was due to an imbalance in the shear and cold pool. The cold pool repeatedly became too strong for the shear, and the low levels of the storm were disrupted as the storm "gusted out". Deep-layer shear was sufficient to help the storm regain organized structure, but not sufficient to overcome the size of the cold pool and allow the storm to attain a steady-state structure.

5. ACKNOWLEDGMENTS

The author would like to thank John Jannuzzi, MIC NWS Boise, for support with this project, and Les Colin and Tim Barker, NWS Boise, for help with this manuscript.

6. REFERENCES

Burgess, D.W., R.R. Lee, S.S. Parker, and D.L. Floyd, 1995: A study of mini supercells observed by WSR-88D radars. *Preprints, 27th Conference on Radar Meteorology*, Vail, CO, Amer. Meteor. Soc., 4-6.

Hurlbut, M. M., and Parker, S. S. 2006: Severe weather threat discrimination in southeast Oregon and southwest Idaho using pre-storm environmental data. Preprints, 23rd Conf. Severe Local Storms, St. Louis MO, Amer. Meteor. Soc., CD-ROM.

More info at http://www.wrh.noaa.gov/boise/SP2010.htm